Numerical Modelling of Dynamic Loss in HTS Coated Conductors under Perpendicular Magnetic Fields

Quan Li, Min Yao, Zhenan Jiang, Chris W Bumby and Naoyuki Amemiya

Abstract— High T_c superconducting (HTS) coated conductors are a promising option for the next generation power devices. However, their thin film geometry incurs dynamic loss when exposed to a perpendicular external AC magnetic field, which is difficult to predicate and estimate. In this paper we propose and verify a numerical simulation model to predict the dynamic loss in HTS thin coated conductors by taking account of their J_c-B dependence and *I-V* characteristics. The model has been tested on a SuperPower YBCO coated conductor, and we observed a linear increase of dynamic loss along the increasing field amplitude after the threshold field. Our simulation results agree closely with experimental measurements as well as an analytical model. Further, the model can predict the nonlinear increase of dynamic loss at high current, while the analytical model deviates from the measurement results and still shows a linear correlation between the dynamic loss and the external magnetic field. In addition, we have used this model to simulate the distributions of magnetic field and current density when dynamic loss occurs. Results clearly show the flux traversing the coated conductor, which causes dynamic loss. The distributions have also been used to analyse the dynamic loss when the transport current and the magnetic field increases individually while the other factor remains constant. The simulation analysis on dynamic loss is for the first done in this paper, and our results clearly demonstrate how dynamic loss changes and its dependence on transport current and magnetic field.

Index Terms—current distribution, coated conductor, dynamic loss, magnetic field distribution, perpendicular magnetic field

I. INTRODUCTION

DYNAMIC loss occurs when a superconductor carrying DC transport current is exposed to an external alternating magnetic field [1-3]. This is particularly important to HTS coated conductors, which have emerged as a promising option for the next generation power devices such as rotating machines [5-7] as well as associated flux pumps [8-11], fault current limiters [12-14] and power cables [15-18]. However, dynamic

loss is difficult to predicate and estimate, since it only occurs under certain conditions that depend heavily on transport current and external magnetic field. This makes accurate prediction of dynamic loss a critical issue which has a high impact on the thermal stability of HTS devices.

The mechanism of dynamic loss has been explained by [1-4]. Analytical models have been proposed to calculate dynamic loss [3, 19] and experimental work has been done on dynamic loss measurements [20-23]. However, there is still a requirement for accurate modelling of the flux and current distributions within the coated conductor wire when dynamic loss occurs. This is important to explain the physical origins of dynamic loss, and to accurately predict its magnitude.

This paper introduces a numerical model developed for this purpose. By applying this model, we have simulated the dynamic loss of a SuperPower YBCO coated conductor. The modelling results are compared with the calculated values from an analytical approximation, as well as experimental measurements of the same coated conductor. Detailed analyses are presented based on results obtained across a wide range of transport currents and AC magnetic field amplitudes. Furthermore, we have simulated the distributions of magnetic fields and current density within the coated conductor wire, which clearly demonstrates the change of dynamic loss. Through this study, we achieved a numerical model to analyse dynamic loss, the results of which can be used to enable the design of effective and efficient cryogenic cooling systems of HTS applications.

II. NUMERICAL MODELLING

The numerical model was developed using the *T* formulation, which is based upon the current vector potential, *T* [24-26]. Unlike the modelling of bulk superconductors [27-29] The thin-strip approximation of the superconducting layer has been applied, since the HTS coated conductor comprises a thin film (typically ~1μm) of superconducting material, which results in a very high aspect ratio (w/t_s) in an order of 10^3 and the thickness can be neglected [30-34]. The governing equation of the electromagnetic field in a coated conductor is derived from Faraday's law as:

$$-\frac{\partial}{\partial y}\frac{1}{\sigma_{sc}}\frac{\partial T}{\partial y} = -\frac{\partial}{\partial t}\left(\frac{\mu_0 t_s}{2\pi}\int \frac{1}{y-y'}\cdot\frac{\partial T}{\partial y}\mathrm{d}y'\right)-\frac{\partial B_\perp}{\partial t} \tag{1}$$

where *y* is the coordinate in the lateral direction of the coated

conductor, σ is the conductivity, t_s is the thickness of the superconductor layer, and $B_\perp$ is the perpendicular component of the external magnetic field, as shown in Figure 1. The current vector potential T is defined by the current density J as $J = \nabla \times T$. There are two terms on the right side of the equation, of which the first one is the time derivative of the self-magnetic field generated by the transport current given by Biot-Savart's law, and the second one is determined by the external magnetic field.

The superconducting property is determined by the power law E-J characteristic. The equivalent conductivity of the coated conductor is derived by:

$$\sigma_{sc} = \frac{J}{E} = \frac{J_c^n}{E_c} J^{1-n} = \frac{J_c^n}{E_c} (\nabla \times T)^{1-n} \tag{2}$$

where $E_c = 1 \times 10^{-4}$ Vm^{-1}. Ohm's law with this equivalent conductivity is used as the constitutive equation as $J = \sigma_{sc} E$. When a coated conductor carries a DC transport current under an AC magnetic field, the DC current I_t occupies the superconducting layer with width $2iw$ in the centre of the coated conductor, leaving the rest with width $(1-i)2w$ free on both sides [3]. Therefore, the dynamic loss Q can be calculated by:

$$Q = \int_{(1-i)w}^{(1+i)w} JEt_s \mathrm{d}y = \int_{(1-i)w}^{(1+i)w} \frac{J^2}{\sigma_{sc}} t_s \mathrm{d}y \tag{3}$$

where i is the ratio between transport current I_t and critical current I_c.

Figure 1

The current density J is a sheet current as indicated in Figure 1 and its distribution (J profile) along the cross section of the HTS coated conductor can be described as $J(y, t)$ at moment t. The perpendicular magnetic self-field distribution at the same moment, $B_s(y, t)$, can be obtained by Ampere's law:

$$B_s(y,t) = \frac{\mu_0}{2\pi} \int_0^{2w} \frac{J(u,t)\mathrm{d}u}{y-u} \tag{4}$$

and the total magnetic field distribution (B profile) is

$$B_s(y,t) = \frac{\mu_0}{2\pi} \int_0^{2w} \frac{J(u,t)\mathrm{d}u}{y-u} + B_{peak} \sin(2\pi f t) \tag{5}$$

where B_{peak} is the amplitude of the external perpendicular magnetic field and f is the frequency.

III. Experimental Measurement

The experimental system we used to measure the dynamic loss is shown in Figure 2. The system consists of a custom-built AC magnet which generates a uniform dipole AC magnetic

field up to 100 mT peak within the sample region, and a DC current supply that provides 0-300 A to simulate transport current at various load rates. Voltage taps were attached along the wire with a length of 50 mm in between, and the wires were arranged in spiral geometry to cancel introduced induction [35]. A picture of the experimental system is shown in Figure 2(b) including (from left) the AC magnet, a cryogenic container to maintain the operational temperature at 77 K, and the power supply. Time-averaged DC voltages were measured using a Keithley 2182 nano-voltage meter at different transport currents. The voltages along with the corresponding transport currents were used to calculate the dynamic losses. The same set of data was also used to calculate the dynamic resistance of the sample, and the results can be found in [20].

Figure 2

TABLE I Specification of the SuperPower YBCO Coated Conductor

Self-field critical current I_c (A)	105.3
Critical current density J_c ($\times 10^{10}$ A/m^2)	2.63
n-value	22.5
Coated conductor width (mm)	4.0
HTS layer thickness (μm)	1.0
Substrate thickness (μm)	50.0

IV. Results and Analyses

The numerical model was tested on an HTS coated conductor manufactured by SuperPower Inc, which is 4 mm wide comprising a 1 μm thin film of YBCO material. Its self-field critical current I_c is 105.3 A at 77 K on the 1 μV/cm criterion, and n-value is 22.5. The full specification of the HTS coated conductor was listed in Table 1. A wide range of transport current I_t from 10% to 90% I_c was simulated, and an external magnetic field of 26.62 Hz was applied perpendicular to the plain of the HTS coated conductor with a magnitude varying between 0 and 100 mT.

A. Validation of the numerical model

The simulation results, along with the measurement results, are presented in Figure 3, in which the dynamic losses are normalised by the length of the HTS coated conductor, so that all the data obtained from simulation and measurement are comparable. Figure 3 also plots the calculated values in solid black lines based on an analytical method derived from [19, 20] as the equation below:

$$Q = \frac{2wfLI_t^2}{I_C}(B_\perp - B_{th}) \tag{6}$$

where f is frequency of the external magnetic field, L is length of the coated conductor (unit length in this paper), $B_\perp$ is the perpendicular external magnetic field, and B_{th} is the threshold field, which is given by:

$$B_{th} = B_p \left(1 - \frac{I_t}{I_C} \right) \quad (7)$$

where B_p is the effective penetration field of the coated conductor [36, 37], and I_t / I_c is the load rate of the coated conductor. B_p is determined by the B value at the maxima of the Γ curve defined by $\Gamma = Q_{BI}/B^2$, where Q_{BI} is Brandt expression for the theoretical magnetization loss in a superconducting thin film exposed to an AC magnetic field [38]. The maxima of this curve can be obtained as:

$$B_p = 2.4642 \frac{\mu_0 J_C t_s}{\pi} \quad (8)$$

where J_c is current density determined by $I_c/(wt_s)$ and t_s is the thickness of the superconducting layer.

Figure 3

At transport currents between 10% and 50% I_c as presented in Figure 3(a), (b) and (c), it can be clearly observed that the simulation results, the measurements and the analytical expression show close agreement throughout the range of the tested magnetic field. The dynamic loss follows a linear correlation with the amplitude of the external magnetic field after the threshold field B_{th}, which is in accordance with the results presented by [21, 23, 39]. Both the analytical expression and the numerical model can predict the onset of dynamic loss correctly, and depict the loss increase accurately.

At higher transport currents of 70% and 90% I_c in Figure 3(d) and (e), the dynamic loss maintains its linear increase after the threshold field, but deviates from this linear correlation and increases rapidly at high field amplitudes. This can be clearly observed at the transport current of 70% I_c when the magnetic field amplitude rises above 80 mT, and at 90% I_c above 40 mT. The rapid increase arises due to the field dependence of the critical current density J_c (B). In this case, the conductor I_c is temporarily reduced below the DC transport current for a short period of each cycle and flux flow loss arises leading to a rapid increase of the dissipated power [20, 40]. The analytical expression (equation 6) doesn't describe this nonlinear increase, since it doesn't include the influence of the field dependent J_c (B). Consequently its result is always linear to the field amplitude, as demonstrated by the black solid lines in Figure 3. By considering the field dependent J_c (B), our numerical model can effectively simulate the rapid increase of the dynamic loss. At 90% I_c, through simulation we found that the dynamic loss nearly doubles when B increases by 10 mT from 40 mT, then doubles again within the next 10 mT increase. Measurement results are a little smaller than simulation since the n-value of the sample may drop in strong magnetic fields, but the patterns of nonlinear increase are in accordance. Experimental data beyond this point are not available, since this rapid increase of loss risks 'burning out' the samples, which did happen during our measurements. Therefore, the numerical model is of special importance under this extreme condition, when experimental measurement is difficult, or even impossible, to carry out.

B. B and J Profiles

Distributions of magnetic field (B profiles) and current density (J profiles) of the HTS coated conductor can be obtained from the numerical model using Equation 5. One example is presented in Figure 4, when the coated conductor is carrying a transport current of 50% I_c in an AC magnetic field of $B = B_{peak} \sin(2\pi ft)$ with $B_{peak} = 20$ mT. B and J profiles are plotted for the two specific moments when the external magnetic field reaches its positive and negative peak values ($B = +B_{peak}$ in dash-dot lines, and $B = -B_{peak}$ in solid lines). The enclosed area between these curves represents the hysteretic flux change within one cycle of the periodic B curve. In addition, the B and J profiles in the absence of an AC external magnetic field are plotted in dash lines as a reference. The B profiles obtained from our numerical model agree closely with the theoretical expression in [41]. During each cycle, the magnetic flux within the shadowed area between the two B profiles travels from region (1) to (2) when the magnetic field increases from $-B_{peak}$ to $+B_{peak}$, then further travels from region (2) to (3) when B drop backs to $-B_{peak}$. Eventually, the flux traverses the HTS coated conductor and causes dynamic loss. The width of the shadowed area is proportional to the transport current, and it is 50% of the total width $2w$ in the case of 50% I_c.

Figure 4

The J profile shows that the DC current is flowing within the shadowed area, which maps the effective region of the HTS coated conductor to carry the transport current I_t. The rest of the HTS coated conductor is occupied by shielding currents induced by the external AC magnetic field. The DC current profile includes variations arising due to field dependent J_c (B) and the increased magnetic field causes a reduction in J_c, which can be observed at either edge of the coated conductor. The B and J profiles obtained from simulation enable clear observation and explanation of dynamic loss.

C. Dependence of Dynamic Loss: Current Effect and Field Effect

Both magnetic field and transport current can heavily influence dynamic loss [1, 2], which we describe here as 'field effect' and 'current effect' for discussion. We simulated the HTS coated conductor at various conditions and found that both effects can be clearly observed and explained by using B and J profiles.

Figure 5
Figure 6

Figure 5 shows the B and J profiles of the HTS coated conductor carrying a constant transport current of 10% I_c, whilst exposed to a magnetic field of different amplitudes, B_{peak}. It is easy to notice that when B_{peak} increases, the B profiles (dash-dot line and solid line) are driven further apart, resulting

in an increase of the area enclosing the amount of traversing flux. The J profiles are almost identical at increasing field amplitudes, with the current density gradually decreased due to the field dependent $J_c (B)$. Together, B and J profiles explain the field effect: dynamic loss increases, because more flux traverses the coated conductor when the external magnetic field increases, even though the coated conductor carries the same current. It is worth mentioning that although the B profiles are displaced further apart at higher field amplitudes, their individual shapes remain nearly identical, because they are essentially determined by the J profiles (self-magnetic field) which don't change much.

Figure 6 shows the B and J profiles of the same coated conductor carrying different transport currents, whilst exposed to the same magnetic field. In this case, the B profiles are not driven apart but shifted away from each other due to the increasing current. The enclosed area increases and contains more traversing flux. Meanwhile, J profiles change due to the increasing transport current. Consequently, the current effect involves both increases of flux and current, which result in a faster increase of dynamic loss compared to the field effect as illustrated by Figure 3.

V. CONCLUSION

Dynamic loss in an HTS coated conductor is difficult to predict, since it only exists under certain conditions which heavily depend on both DC transport current and AC magnetic field. For the first time, we have developed a numerical model employing T formulation which enables the accurate simulation of dynamic loss in a perpendicular magnetic field, and shows close agreement with experimental results. At high transport current of 90% I_c and high external magnetic field above 40 mT, the model can accurately depict the nonlinear rapid increase of the dynamic loss, which arises due to flux-flow loss as $I_c (B_{peak})$ falls below I_t.

The model can also calculate the distributions of magnetic field and current density within the coated conductor wire. We obtained these distributions for an HTS coated conductor at 50% I_c at 20 mT, which can clearly show the magnetic flux traversing the coated conductor that causes dynamic loss. In addition, we used the model to simulate an HTS coated conductor (i) carrying constant current in different magnetic fields and (ii) carrying different current in the same field. Results show that the amount of flux traversing the coated conductor increases in both cases, but due to the increasing field and current respectively. These results clearly demonstrate the change of dynamic loss and its dependence on transport current and magnetic field.

REFERENCES

[1] V. Andrianov, V. Zenkevitch, V. Kurguzov, V. Sytchev and F. Ternovskii, "Effective resisitance of a type 2 non-ideal superconductor in an oscillating magnetic field," *Sov. Phys. JETP*, vol. 31, p. 815, 1970

[2] T. Ogasawara, K. Yasukochi, S. Nose and H. Sekizawa, "Effective resistance of current-carring superconducting wire in oscillating magnetic fields 1: Single core composite conductor," *Cryogenics*, vol. 16, no. 1, pp. 33-38, 1976

[3] M. P. Oomen, J. Rieger, M. Leghissa, B. ten Haken and H. H. J. ten Kate, "Dynamic resistance in a slab-like superconductor with $J_c(B)$ dependence," *Supercond. Sci. Technol.*, Vol. 12, pp. 382-387, 1999

[4] F. Sumiyoshi and K. Funaki, "Superconducting multi-filamentary wires and conductors," *Sanyo, Tosho* Japan 1995

[5] A. Gonzalez-Parada, F. Trillaud, R. Guzman-Cabrera and M. Abatal, "Torque ripple reduction in an axial flux high temperature superconducting motor," *IEEE Trans. Appl. Supercond.* vol. 25, 5202805, 2015

[6] T. Nishimura, T. Nakamura, Q. Li, N. Amemiya and Y. Itoh, "Potential for torque density maximization of HTS induction/synchronous motor by use of superconducting reluctance torque," *IEEE Trans. Appl. Supercond.* vol. 24, 5200504, 2014

[7] S. Baik, Y. Kwon, S. Park and H. Kim, "Performance analysis of a superconducting motor for higher efficiency design," *IEEE Trans. Appl. Supercond.* vol. 23, 5202004, 2013

[8] Z. Jiang, K. Hamilton, N. Amemiya, R. Badcock and C. W. Bumby, "Dynamic resistance of a high-T_c superconducting flux pump," *Appl. Phys. Lett.*, vol. 105, 112601, 2014

[9] C. W. Bumby, Z. Jiang, J. G. Storey, A. E. Pantoja and R. Badcock, "Anomalous open-circuit voltage from a high-Tc superconducting dynamo," *Appl. Phys. Lett.*, vol. 108, 122601, 2016

[10] Z. Jiang Z, C. W. Bumby, R. Badcock, H. J. Sung, N. J. Long and N. Amemiya, "Impact of flux gap upon dynamic resistance of a rotating HTS flux pump," *Supercond. Sci. Technol.*, vol.28, 115008, 2015

[11] C. W. Bumby, R. Badcock, H. J. Sung, K. M. Kim, Z. Jiang, A. E. Pantoja, P. Bernardo, M. Park and R. G. Buckley, "Development of a brushless HTS exciter for a 10 kW HTS synchronous generator," *Supercond. Sci. Technol.*, vol. 29, 024008, 2016

[12] Z. Wei, Y. Xin, J. Jin and Q. Li, "Optimized design of coils and iron cores for a saturated iron core superconducting fault current limiter," *IEEE Trans. Appl. Supercond.*, vol. 26, 5603904, 2016

[13] P. Pascal, A. Badel, G. Auran and G. Santos Pereira, "Superconducting fault current limiter for ship grid simulation and demonstration," *IEEE Trans. Appl. Supercond.*, vol. 27, 5601705, 2017

[14] J. Kozak, M. Majka and S. Kozak, "Experimental results of a 15 kV, 140 A superconducting fault current limiter," *IEEE Trans. Appl. Supercond.*, vol. 27, 5600504, 2017

[15] Q. Li, N. Amemiya, K Takeuchi, T Nakamura and N Fujiwara, "AC Loss Characteristics of Superconducting Power Transmission Cables: Gap Effect and Jc Distribution Effect," *Supercond. Sci. Technol.*, vol. 23, 115003, 2010.

[16] Q. Li, N. Amemiya, R. Nishino, T. Nakamura and T. Okuma, "AC Loss Reduction of Outer-Diameter-Fixed Superconducting Power Transmission Cables using Narrow Coated Conductors," *Physica C*, vol. 484, pp. 217-222, 2013.

[17] N. Amemiya, Q. Li, K. Ito, K. Takeuchi, T. Nakamura and T. Okuma, "AC Loss Reduction of Multilayer Superconducting Power Transmission Cables by Using Narrow Coated Conductors," *Supercond. Sci. Technol.*, vol. 24, 065013, 2011.

[18] Z. Jiang, N. Long, M. Staines, Q. Li, R. Slade, N. Amemiya and A. Caplin, "Transport AC Loss Measurements in Single- and Two-Layer Parallel Coated Conductor Arrays with Low Turn Numbers," *IEEE Trans. Appl. Supercond.*, vol. 22, no. 3, 8200306, 2012

[19] T. Matsushita, 1994 *Flux pinning and electromagnetic phenomenon* (Sangyo Tosho Inc. Tokyo) pp 99.

[20] Z. Jiang, R. Toyamoto, N. Amemiya, X. Zhang and C. W. Bumby, "Dynamic resistance of a high-T_c superconducting trip in perpendicular magnetic field," *Supercond. Sci. Technol.*, vol. 30, 03LT01, 2017.

[21] M. Ciszek, O. Tsukamoto, J. Ogawa, and D. Miyagi, "Energy losses in YBCO-123 coated conductors carrying transport current in perpendicular external magnetic field," *AIP Conf. Proc.*, vol. 614, pp. 606-613, 2002.

[22] R. C. Duckworth, Y. F. Zhang, T. Ha, and M. J. Gouge, "Dynamic resistance of YBCO-coated conductors carrying transport current in perpendicular external magnetic field," *IEEE Trans. Appl. Supercond.*, vol. 21, pp. 3251-3256, 2011.

[23] Z. Jiang, R. Toyamoto, N. Amemiya, C. W. Bumby, R. Badcock and N. Long, "Dynamic resistance measurements in a GdBCO-coated conductor," *IEEE Trans. Appl. Supercond.*, vol. 27, 5900205, 2017.

[24] C. J. Carpenter, "Comparison of alternative formulations of 3-dimensional magnetic-field and eddy-current problems at power frequencies," *Proc. IEE*, vol. 124, pp. 1026-1034, 1977.

[25] T. W. Preston and A. B. J. Reece, "Solution of 3- Dimensional Eddy Current Problems: The T-Sl Method," *IEEE Trans. Magn.*, vol. 18, pp. 486-491, 1982.

[26] T. Nakata, N. Takahashi, K. Fujiwara and Y. Okada, "Improvements of the T-Omega method for 3-D eddy current analysis," *IEEE Trans. Magn.*, vol. 24, pp. 94-97, 1988.

[27] Q. Li, Y. Yan, C. Rawlings and T. Coombs, "Magnetization of Bulk Superconductors Using Thermally Actuated Magnetic Waves," *IEEE Trans. Appl. Supercond.*, vol. 20, no. 3, pp. 2243-2247, 2010.

[28] Q. Li, Y. Yan, C. Rawlings and T. Coombs,, "Numerical Analysis of Thermally Actuated Magnets for Magnetization of Superconductors," *J. Phys.: Conf. Ser.*, vol. 234, 032035, 2010.

[29] Y. Yan, Q. Li and T. Coombs, "Thermally Actuated Magnetization Flux Pump in Single-Grain YBCO Bulk," *Supercond. Sci. Technol.*, vol. 22, 105001, 2009.

[30] Y. Ichiki and H. Ohsaki, "Numerical analysis of AC losses in YBCO coated conductor in external magnetic field," *Physica C*, vol. 412-414, pp. 1015-20, 2004.

[31] E. Pardo, "Modelling of AC loss in coils made of thin tapes under DC bias current," *IEEE Trans. Appl. Supercond.*, vol. 24, 4700105, 2014.

[32] Q. Li, H. Tan and X. Yu, "Effect of Multilayer Configuration on AC Losses of Superconducting Power Transmission Cables Consisting of Narrow Coated Conductors," *IEEE Trans. Appl. Supercond.*, vol. 24, no. 3, 5400604, 2014.

[33] Q. Li, N. Amemiya, K. Takeuchi, T. Nakamura and N. Fujiwara, "Effects of Unevenly Distributed Critical Currents and Damaged Coated Conductors to AC Losses of Superconducting Power Transmission Cables," *IEEE Trans. Appl. Supercond.*, vol. 21, no. 3, pp. 953-956, 2011.

[34] N. Amemiya N, Q. Li, R. Nishino, K. Takeuchi, T. Nakamura, K. Ohmatsu, M. Ohya, O. Maruyama, T. Okuma and T. Izumi, "Lateral Critical Current Density Distributions Degraded near Edges of Coated Conductors through Cutting Processes and their Influence on AC Loss Characteristics of Power Transmission Cables," *Physica C*, vol. 471, pp. 990-994, 2011.

[35] S. Fukui, Y. Kitoh, T. Numata, O. Tsukamoto, J. Fujikami, and K. Hayashi, "Transport current AC losses of high-T_c superconducting tapes exposed to AC magnetic field," *Adv. Cryogenic. Eng.*, vol. 44, pp. 723-730, 1998.

[36] M. Iwakuma, K. Toyota, M. Nigo, T. Kiss, K. Funaki, Y. Iijima, T. Saitoh, Y. Yamada, and Y. Shiohara, "AC loss properties of YBCO superconducting tapes fabricated by IBAD-PLD technique," *Physica C*, vol. 412-414, pp. 983-991, 2004.

[37] A. Palau, T. Puig, X. Obradors, E. Pardo, C. Navau, A. Sanchez, A. Usoskin, H. C. Freyhardt, L. Fernández, B. Holzapfel, and R. Feenstra, "Simultaneous inductive determination of grain and intergrain critical current densities of YBa2Cu3O7-x coated conductors," *Appl. Phys. Lett.*, vol. 84, pp. 230-232, 2004.

[38] E. H. Brandt and M. Indenbom, "Type-II superconductor strip with current in a perpendicular magnetic field," *Phys. Rev. B*, vol. 43, 12893, 1993.

[39] M. Ciszek, H. G. Knoopers, J. J. Rabbers, B. ten Haken, and H. H. J. ten Kate, "Angular dependence of the dynamic resistance and its relation to the AC transport current loss in Bi-2223/Ag tape superconductors," *Supercond. Sci. Technol.*, vol. 15, pp. 1275-1280, 2002.

[40] A. Uksusman, Y. Wolfus, A. Friedman, A. Shaulov, and Y. Yeshurun, "Voltage response of current carrying YBaCuO tapes to alternating magnetic fields," *J. Appl. Phys.*, vol. 105, 093921, 2009.

[41] G. P. Mikitak and E. H.. Brandt, "Generation of a DC voltage by an AC magnetic field in type-II superconductor," *Phys. Rev B*, vol. 64, 092502, 2001.
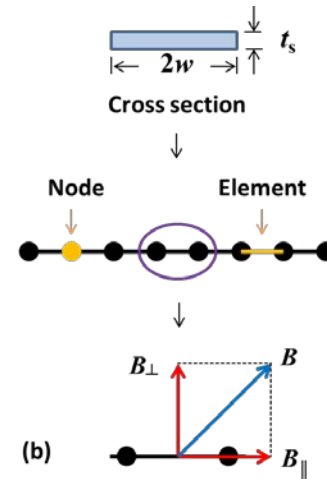
Fig. 1. (a) Transport current *J*, magnetic field *B*, and definition of coordinates of a HTS coated conductor, and (b) modelling of the HTS coated conductor under magnetic field *B* along its cross section (width: $2w$, thickness: t_s).
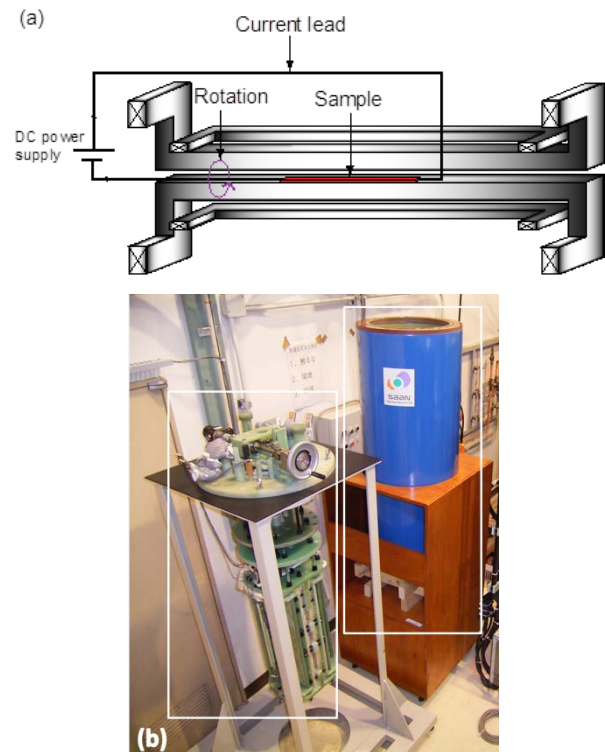
Fig. 2. (a) Schematic of the experimental system for the measurement of dynamic loss in an HTS coated conductor, and (b) picture of the system with an AC magnet and an sample holder (left), and a cryogenic container (right).
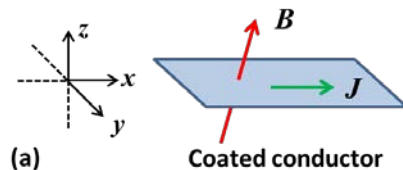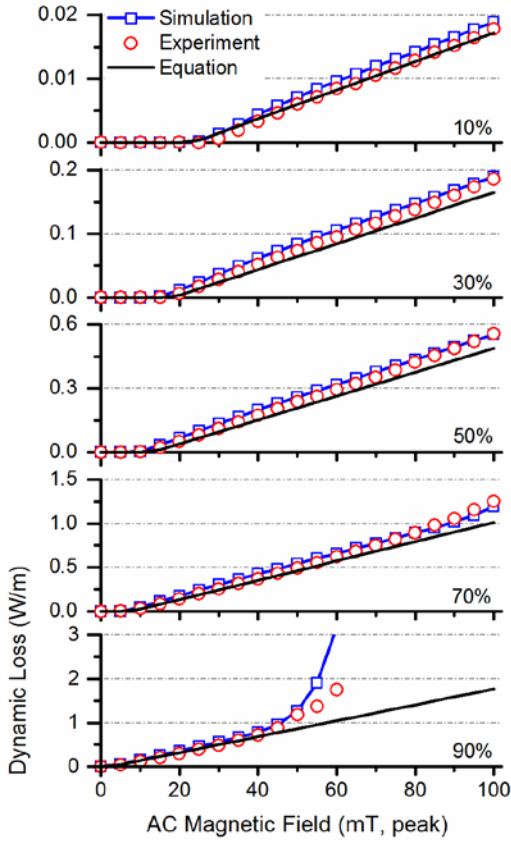
Fig. 3. Comparison of the dynamic losses between experimental measurements, numerical simulation, and analytical expression of Equation (6). The load rate (I_t/I_c) is set at (from top to bottom) 10%, 30%, 50%, 70%, and 90%. An AC magnetic field was applied at 26.62 Hz from 0 to 100 mT.
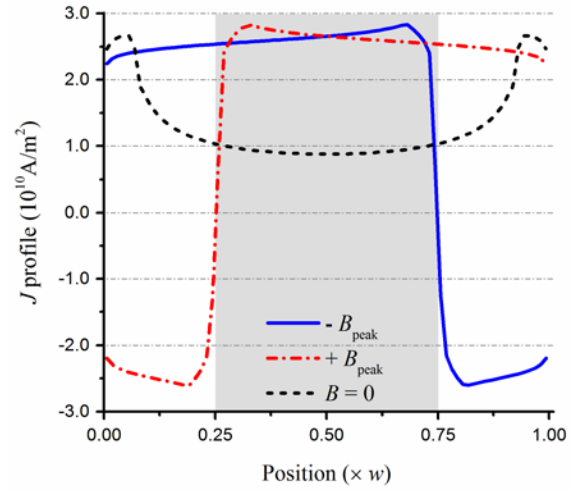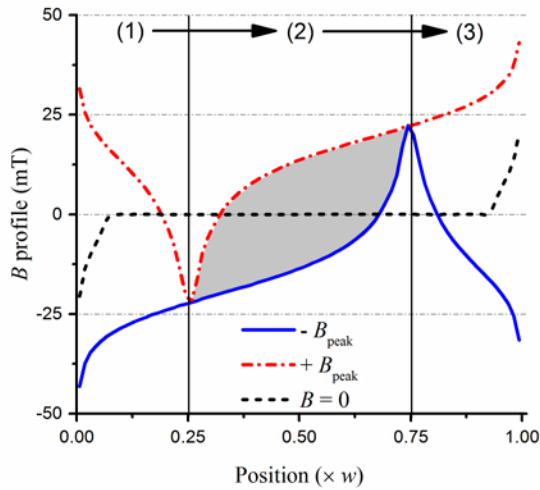
Fig. 4. (a) Distribution of magnetic field (B profile) and (b) distribution of current density (J profile) of an HTS coated conductor, at the transport current of 50% I_c under a magnetic field of $B = B_{peak} \sin(wt)$ with $B_{peak} = 20$ mT. The solid lines (blue) are obtained when the external magnetic field reaches its negative peak ($B = -B_{peak}$), and the dash-dot lines (red) are at the positive peak ($B = +B_{peak}$), with the dash lines (black) at $B_{peak} = 0$ (no external magnetic field) as reference. The shadowed part in (a) indicates the area that contains the magnetic flux traversing from region (1) through (2) to (3), which maps the shadowed belt in (b) where DC current flows and dynamic loss occurs.
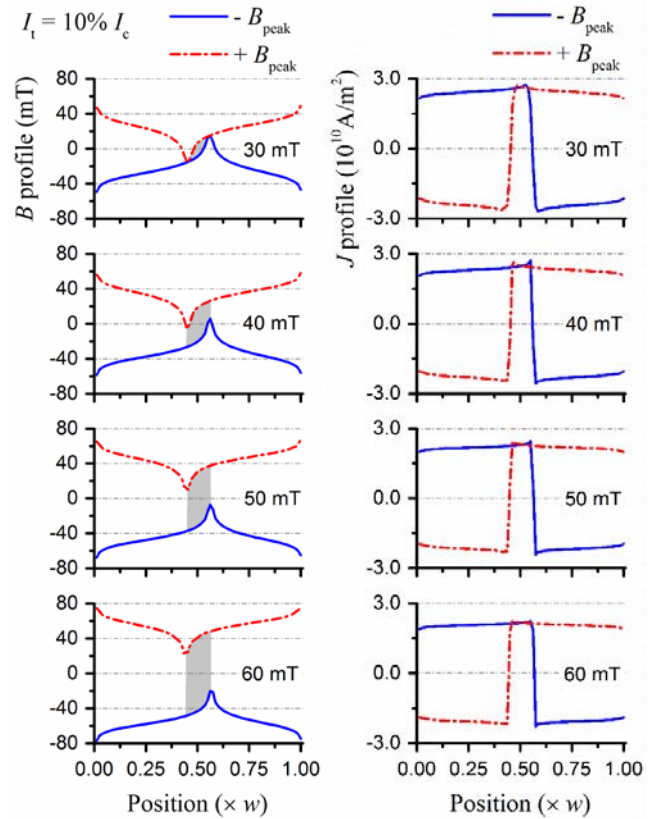
Fig. 5. B and J profiles of an HTS coated conductor carrying a constant transport current of 10% I_c, whilst exposed to a magnetic field of different amplitudes, $B_{peak} = 30{\sim}60$ mT. Definitions of lines and shadowed areas are the same as Figure 4.
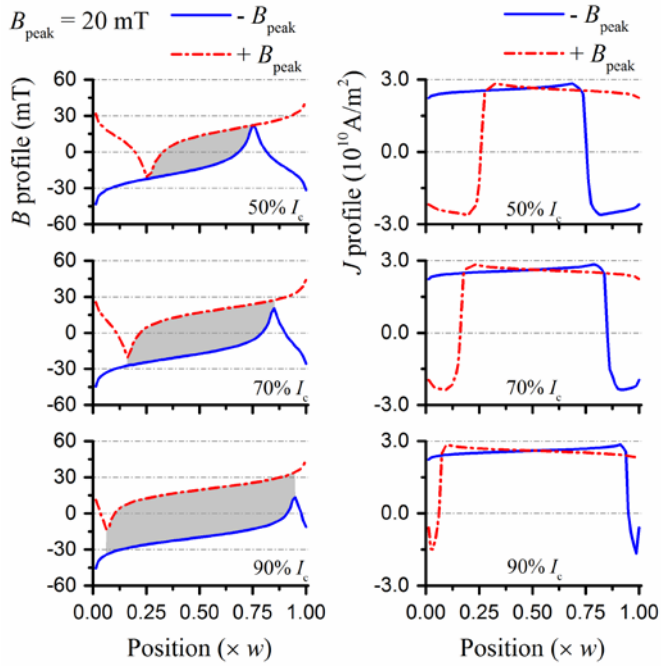
Fig. 6. *B* and *J* profiles of an HTS coated conductor carrying different transport currents I_t = 50%~90% I_c, whilst exposed to the same magnetic field, B_{peak} = 20 mT. Definitions of lines and shadowed areas are the same as Figure 4.